JOURNAL OF CHEMICAL INFORMATION AND MODELING

Article

pubs.acs.org/jcim

How Does Catalase Release Nitric Oxide? A Computational Structure−Activity Relationship Study

Sai Lakshmana Vankayala, Jacqueline C. Hargis, and H. Lee Woodcock*

Department of Chemistry, University of South Florida, 4202 E. Fowler Avenue, CHE205, Tampa, Florida 33620-5250, United States

Supporting Information

ABSTRACT: Hydroxyurea (HU) is the only FDA approved medication for treating sickle cell disease in adults. The primary mechanism of action is pharmacological elevation of nitric oxide (NO) levels which induces propagation of fetal hemoglobin. HU is known to undergo redox reactions with heme based enzymes like hemoglobin and catalase to produce NO. However, specific details about the HU based NO release remain unknown. Experimental studies indicate that interaction of HU with human catalase compound I produces NO. Presently, we combine flexible receptor−flexible substrate induced fit docking (IFD) with energy decomposition analyses to examine the atomic level details of a possible key step in the clinical conversion of HU to NO. Substrate binding modes of nine HU analogs with catalase compound I were investigated to determine the essential properties necessary for effective NO release. Three major binding orientations were found that provide insight into the possible reaction mechanisms for producing NO. Further results show that anion/radical intermediates produced as part of these mechanisms would be stabilized by hydrogen bonding interactions from distal residues His75, Asn148, Gln168, and oxoferryl-heme. These details will ideally contribute to both a clearer mechanistic picture and provide insights for future structure based drug design efforts.

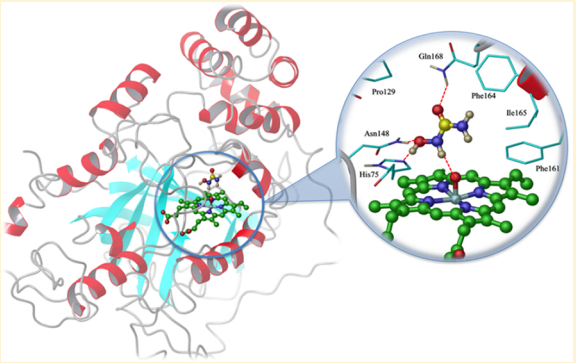

1. INTRODUCTION

Sickle cell disease (SCD), an inherited monogenic disorder, results from the mutation of the sixth amino acid in the β-globin gene changing from the polar amino acid glutamic acid to the nonpolar residue valine.[1] This mutation forms defective, sickled hemoglobin (HbS). Upon deoxygenation, HbS undergoes polymerization into long fibrils that ultimately results in "sickled" red blood cells. Symptoms of SCD are intense pain, microvascular vaso-occlusion, acute chest syndrome, stroke, severe multiorgan damage, and even death.[2−4]

In 1998, the FDA approved hydroxyurea (HU) as a SCD treatment,[5] and it remains the only remedy for severe cases.[6] HU, a known nitric oxide (NO) source, induces fetal hemoglobin (HbF) production, which is largely responsible for mitigating sickle cell severity.[7,8] HbF synthesis is controlled by γ-globin gene expression, which is believed to be upregulated via the activation of the NO dependent soluble guanylyl cyclase (sGC) pathway in human erythroid progenitor cells.[9,10] In addition to HU's role in HbF production, the NO derived from its conversion also assists in maintaining normal blood pressure, smoothening muscles, producing relaxation, and improving blood flow to assist patients with intense pain resulting from inflammation. Increased NO bioavailability also improves red cell rheological properties and endothelial cell interactions. Moreover, HU ameliorates antioxidant defense by decreasing lipid peroxidation levels by at least 30% due to its contribution to higher catalase activity in SCD patients.[11] SCD patients undergoing HU therapy are known to produce various intermediates like C-nitroso formamide, nitroxyl, nitric oxide, nitrates, and nitrites, which have numerous human physiological effects.[12]

A 2004 study by King and co-workers[13] showed that HU interacts with oxy-hemoglobin (oxyHb) and deoxy-hemoglobin (deoxyHb) resulting in slow NO production rates. This did not correlate with the observed increase in NO concentrations in patients undergoing HU therapy. The discrepancy can be attributed to the interaction of HU with competing heme based enzymes[13−17] such as catalase, other human globins, and peroxidases that are also known to produce NO. Elucidation of the molecular level interactions between HU and each of these heme based enzymes is critical to understanding NO metabolite concentrations in patients undergoing HU therapy. Specifically, hydroxyurea analogs, (HUA, Figure 1) previously established to be a good diversity set through interaction with hemoglobin,[17,18] will be used for the present computational structure−activity relationship (SAR) study with catalase.

Catalase enzymes are typically classified into three subtypes: monofunctional catalases, bifunctional catalase peroxidases, and pseudo catalases.[19] Monofunctional catalases, known as mammal catalases, are commonly present in animals. Their quaternary structures are similar across organisms and are

Received: July 7, 2013
Published: October 3, 2013

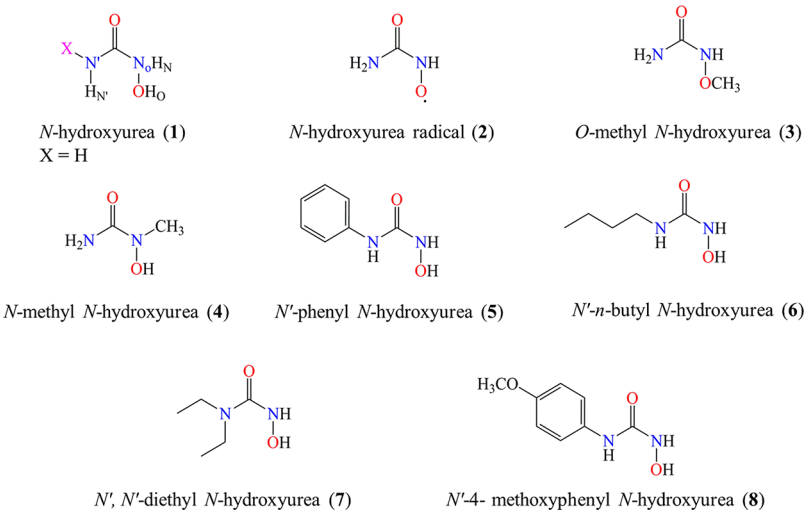

Figure 1. Hydroxyurea analogs tested for their structure−activity relationship by King and co-workers in hemoglobin. The specific nomenclature used for different hydrogen and nitrogen atoms is the following: nonhydroxyl nitrogen atom (N′), nitrogen attached to hydroxyl moiety (N_O), hydrogen atom bonded to N′ atom ($H_{N'}$), hydrogen bonded to N_O atom (H_N), hydroxyl hydrogen as (H_O), and substituent alkyl/phenyl groups bonded to the nonhydroxyl nitrogen atom (X). Hydroxyurea as a generic model to define the nomenclature.

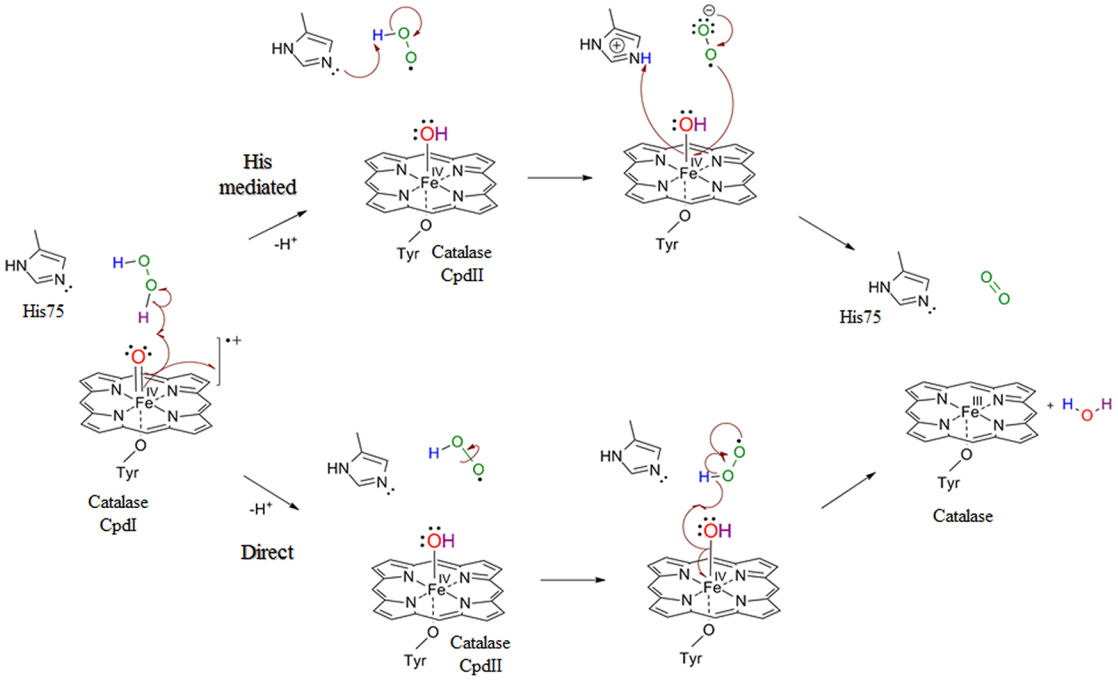

Figure 2. Proposed mechanisms of action for the breakdown of H_2O_2 by catalase CpdI: His mediated (top) and direct mechanism (bottom).

generally present as a tetramer with four equal subunits consisting of a hydrophobic pocket that strongly binds heme prosthetic groups. The catalase heme group exists as a pentavalent coordinated system with ferric iron having four coordinate bonds to porphyrin nitrogens while the fifth bond is to the proximal tyrosine. Compared to most other enzymes, catalases are more resistant to pH change and thermal denaturation due to their stable tetrameric interactions.[20] Catalases prevent mutagenesis and apoptosis[19] and promote antioxidant defense mechanisms against reactive oxygen species (ROS)[11,21] to reduce oxidative stress, inflammatory response, and membrane lipid peroxidation levels in SCD patients undergoing HU therapy.

Despite a wide variety of functionality, catalases are primarily known for combating ROS such as hydrogen peroxide (H_2O_2). Ferric catalase (Fe^{III}) protects hemoglobin by dissociating two H_2O_2 molecules sequentially, in normal human erythrocytes, into water and oxygen molecules.[19] The reaction cycle[22] begins with high spin ferric heme interacting with H_2O_2 to form an oxoferryl porphyrin cation radical ($O{=}Fe^{IV}{-}Por^{+\cdot}$), also known as compound I (CpdI). The second H_2O_2 molecule reduces CpdI to its native resting state enzyme. Two possible mechanisms have been proposed for the H_2O_2−catalase CpdI reduction: a histidine (His) mediated mechanism and a direct mechanism. The His mediated mechanism, proposed by Fita and Rossmann,[23] is comprised of sequential hydrogen transfer to CpdI with the distal His playing a catalytic role. This differs

dx.doi.org/10.1021/ci400395c | J. Chem. Inf. Model. 2013, 53, 2951−2961

from the direct mechanism proposed by Kato and co-workers,[24] where the hydrogen atoms are successively transferred from H_2O_2 to the oxoferryl group in the active site with His only playing substrate recognition and stabilization roles (Figure 2).

In an attempt to verify and characterize the catalase catalyzed conversion of HU to NO, King and co-workers performed a series of electron paramagnetic resonance (EPR) spectroscopic studies.[12,13,15] Figure 3 illustrates their findings. The catalase

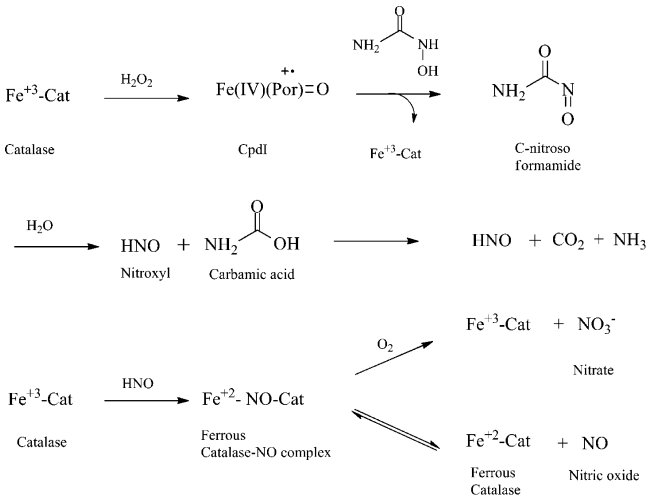

Figure 3. Generic representation of the catalase mediated NO production from hydroxyurea proposed by King and co-workers. The reaction step shows the C-nitroso formamide intermediate, a necessary precursor for NO formation.

mediated NO reaction begins with the production of CpdI, identical in mechanism to H_2O_2. CpdI then interacts with HU to produce C-nitroso formamide followed by the formation of nitroxyl (HNO) upon hydrolysis. Subsequently, HNO interacts with native ferric catalase to generate a ferrous NO-catalase complex, which serves as a source of NO. The released NO was monitored by an oxyHb assay and EPR spectroscopic trapping experiments.[13] Despite this information, the detailed mechanism of action remains unclear due to the lack of a 3D bioactive crystal structure. Herein, we seek a greater understanding of the atomistic interactions between catalase CpdI and the HU analog diversity set by a combination of flexible receptor−flexible substrate induced fit docking (IFD), structure and sequence based bioinformatics, and quantum mechanical (QM) calculations.

2. COMPUTATIONAL DETAILS

X-ray crystal structure coordinates of catalase were obtained from the protein data bank [PDB: 1DGG].[25] 1DGG is a high resolution, 1.5 Å, tetramer containing NADPHs, heme prosthetic groups, and bound cyanide. The prosthetic heme iron exists in the hexa coordinate state. The NADPH region is hydrated; whereas the immediate active site and β-barrel regions are devoid of structural waters. Chain A of PDB 1DGG was used, and the cyanide group was manually back mutated to an oxygen atom with an Fe=O bond length of 1.71 Å along with incrementing the charge on iron to +4 to replicate CpdI.[26] The IMPACT molecular mechanics program[27] was used to correct bond orders, add missing hydrogens, and remove cocrystallized water molecules not present in the active site. The histidine protonation state HSD (protonated on $N_{\delta 1}$ only) was selected for His75 corresponding to both the His mediated and direct mechanisms proposed previously.[23,24] A Truncated Newton Conjugate Gradient (TNCG) minimization was performed using the OPLS-2005 force field. The oxoferryl-heme was frozen in a constant dielectric of 2. All substrate structure atomic coordinates were built and minimized using Schrödingers LigPrep 2.3[28] module before preliminary docking investigations.

Enzyme flexibility is a key component in determining receptor/substrate recognitions. Flexible receptor−flexible ligand docking, also known as induced fit docking (IFD),[29,30] was used to characterize conformational changes in catalase CpdI upon HUA binding. The IFD protocol uses a combination of Glide (Grid-base ligand docking with energetics)[31] rigid docking with protein structure prediction (Prime).[29] This methodology has been well-validated and successfully applied to various biological problems including loop predictions,[32,33] homology modeling,[34] fragment based docking,[35] and enrichment studies.[36,37] The various steps implemented in sequential order during the IFD protocol are described below:

(1) Active site residues mutated to Ala: All side chains within 8 Å of the oxoferryl oxygen were mutated to alanine. The distal His75 was excluded from this process as it is essential to structural integrity.

(2) Rigid docking: Docking of HUAs was performed by GlideSP (Glide standard precision)[38] against the mutated catalase CpdI structure with an increased Coulomb−vdW nonbonded interaction energy cutoff of 100 kcal mol^{-1} to generate more poses. Additionally, vdW radii were scaled by a factor of 0.5 for the ligand and 0.7 for the receptor to generate an initial ensemble of docked poses with reduced steric clashes. Also, 300 poses of partially optimized receptor−substrate complexes were requested.

(3) Protein refinement: The GlideSP docked complexes were refined using prime's structure prediction tool and the OPLS-2005 force field with generalized Born solvation.[39−41] Alanine residues were back-mutated to their initial amino acids. By default, IFD uses a three step procedure to sample side chain conformations and predict ligand−residue orientations: (a) Rotamer libraries developed by Xiang and Honig[41] were used to generate side chain conformations. All previously mutated side chains were back mutated simultaneously into a random rotamer state obtained from the aforementioned library. (b) Each side chain was minimized sequentially. This procedure involves minimization of a single side chain (<0.001 kcal mol^{-1} $Å^{-1}$ rms gradient) while keeping all others fixed. This was repeated sequentially for all back mutated residues until convergence is reached. (c) Finally, a TNCG minimization with full vdW radii was performed to resolve any remaining steric clashes.

(4) Redocking: The substrates within a 40 kcal mol^{-1} energy window of the lowest energy structure from the refinement step were redocked into the induced fit structures. GlideXP (Glide Extra precision)[31] with full vdW scaling was employed for all docking. 500 poses were requested for the redocking and ranked based on the GlideXP score. All poses were clustered based upon ligand orientation; nonproductive poses are reported in

dx.doi.org/10.1021/ci400395c | J. Chem. Inf. Model. 2013, 53, 2951−2961

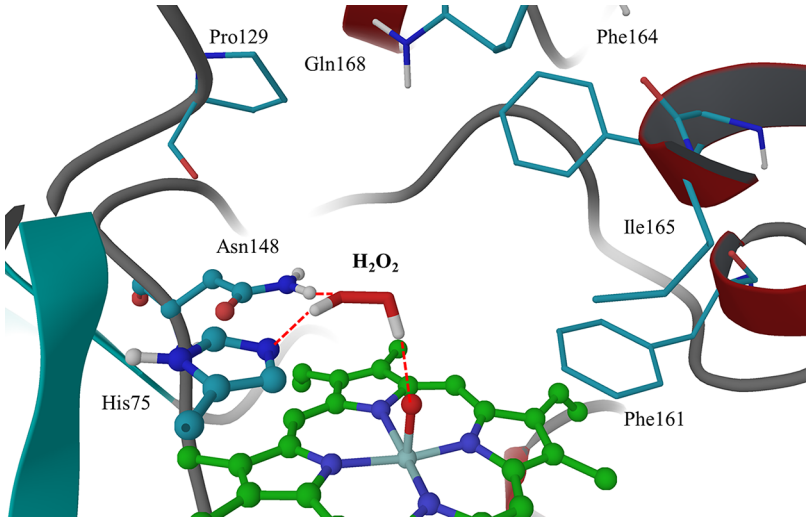

Figure 4. Intermolecular hydrogen bonding network observed for the H_2O_2 docking orientation in the catalase CpdI active site.

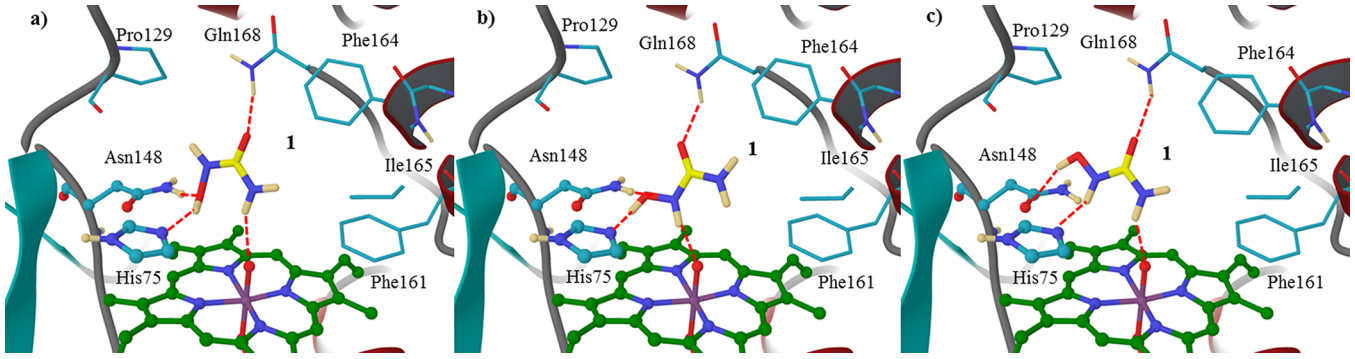

Figure 5. Predicted binding orientations of hydroxyurea (**1**) in catalase CpdI: pose A (a), pose B (b), and pose AB (c).

the Supporting Information (SI) however, not included in subsequent analysis. XP descriptors were generated by fragmenting the composite scoring function into various interaction energies to analyze the docked poses.

This results in nine energies grouped into "reward" and "penalty". The reward term includes: HBond, a generic chemscore hydrogen bonding pair term;[42] PhobEnHb, a hydrogen bond in protein hydrophobic enclosure; PhobEn, a hydrophobic enclosure term; LipophilicEvdW, a chemscore−lipophilic pair term; Electro, an electrostatic contribution; Sitemap, complementary non-hydrogen bonding interactions; and LowMW, a reward for having lower molecular weight. The penalty term consists of the following: RotPenal, a penalty for constricting flexible ligands, and XP Penalties, a collective combination of intraligand contact, polar atom burial, amide torsion, and desolvation. CHARMM[43−45] was used to compute active site side chain rmsds including the 2-fold symmetry of the phenylalanine side chains. Application of the IFD protocol produced an ensemble of catalase CpdI complexes, which were clustered for each HUA. Three dominant clusters were found. Q-Chem 4.0[46,47] at the B3LYP/6-31G* level of theory[48,49] with a 75/302 integration grid was used for all quantum calculations (i.e., investigation of torsional potential as it relates to proposed mechanism, vide infra).

3. RESULTS AND DISCUSSION

The aforementioned HUAs were initially tested by King and co-workers[17] for their efficacy to produce NO while interacting with adult human hemoglobin. Analogs **1**, **5**, **6**, and **8** produce NO due to the presence of an −NHOH group and its adjacent $H_{N'}$ which stabilizes the radical intermediates via a hydrogen bond to Gly25.[18] These binding and reaction mechanisms differ from the present case of catalase CpdI where HUAs must first form C-nitroso formamide intermediates before final NO production. The absence of 3D structures further complicates the elucidation of structure−reaction details of HUAs with CpdI. Herein we examine catalase CpdI substrate specificity with previously used HU derivatives. Interaction energies are analyzed to provide deeper insight into preferential binding modes and possible reactions.

The docking protocol was validated by comparing to a QM/MM optimized H_2O_2−CpdI structure previously published by Alfonso-Prieto et al.[26] The H_2O_2 pose generated using IFD matched the QM/MM minimized structure; particularly the intermolecular hydrogen bond network between the $-NH_2$ of Asn148, the proximal hydroxyl of H_2O_2 (a hydrogen bond donor to His75), the distal hydroxyl of H_2O_2, and the oxoferryl oxygen (Figure 4).

Three predominant pose conformations were obtained for HUAs and were categorized as pose A, pose B, and pose AB. The top scoring poses from each cluster were used for further analysis. All three poses were observed for HUAs **1**, **5**, **6**, and **8**,

dx.doi.org/10.1021/ci400395c | J. Chem. Inf. Model. 2013, 53, 2951−2961

Table 1. XP Descriptor Analysis Showing the Contribution of GlideXP Terms (kcal mol^{-1}) for Poses A, B, and AB Conformations of HUAs

title	GScore	HBond	PhobEnHB	PhobEn	LipophilicEvdW	RotPenal	Penalties	Electro	Sitemap	LowMW
1 pose A	−5.1	−2.8	0.0	0.0	−0.5	0.0	0.0	−0.9	−0.4	−0.5
1 pose B	−4.9	−2.8	0.0	0.0	−0.5	0.0	0.1	−0.8	−0.4	−0.5
1 pose AB	−4.1	−1.9	0.0	0.0	−0.5	0.0	0.0	−0.8	−0.4	−0.5
3	−4.0	−1.9	0.0	0.0	−0.4	0.0	0.0	−0.8	−0.4	−0.5
4	−5.5	−2.9	0.0	0.0	−0.8	0.0	0.0	−0.9	−0.4	−0.5
5 pose A	−8.4	−1.9	−1.4	−1.5	−3.0	0.6	0.3	−0.7	−0.2	−0.5
5 pose B	−7.4	−2.8	0.0	−0.9	−2.9	0.6	0.1	−0.6	−0.4	−0.5
5 pose AB	−8.7	−1.6	−1.5	−1.5	−3.0	0.6	0.1	−0.9	−0.3	−0.5
6 pose A	−5.9	−2.8	0.0	−0.8	−2.2	1.4	0.1	−0.7	−0.4	−0.5
6 pose B	−5.9	−2.6	0.0	−0.9	−2.2	1.4	0.1	−1.0	−0.3	−0.5
6 pose AB	−5.0	−1.8	0.0	−0.8	−2.3	1.4	0.2	−0.8	−0.4	−0.5
7 pose B	−2.6	−2.1	0.0	0.0	−1.9	0.7	2.4	−0.8	−0.3	−0.5
8 pose A	−7.4	−2.3	−1.5	0.0	−2.9	0.6	0.4	−0.8	−0.4	−0.5
8 pose B	−5.8	−1.9	0.0	0.0	−3.3	0.6	0.0	−0.6	−0.3	−0.5
8 pose AB	−5.6	−1.5	−0.9	0.0	−3.0	0.6	0.5	−0.6	−0.2	−0.5

while **7** formed only pose B. Neither **3** nor **4** adopted pose A, B, or AB due to the absence of the −NHOH group.

The pose A orientation has the $-NH_2$ of Asn148 donating a hydrogen bond to the HUA hydroxyl group. In turn, the hydroxyl group donates a hydrogen bond to the N_ε of His75. This network continues via the $H_{N'}$ hydrogen bonding to the oxoferryl group of CpdI (Figure 5a). In contrast to pose A, pose B is not stabilized through an interaction with its $H_{N'}$. Instead, the Asn148−substrate−His75/oxoferryl network is exclusively formed via the −NHOH moiety with H_N hydrogen bonding to oxoferryl (Figure 5b). Similar to pose A, pose AB's $H_{N'}$ forms a hydrogen bond with CpdI's oxoferryl group. However, the −NHOH moiety in pose AB has a different hydrogen bonding pattern compared to the previous poses (Figure 5c). The N_ε of His75 accepts a hydrogen bond from H_N, while Asn148's side chain carbonyl accepts H_O as its hydrogen bond donor. Further, all HUA —C═O moieties hydrogen bond with the Gln168 $-NH_2$. XP descriptors of the top scoring poses in catalase CpdI were retained and analyzed (Table 1) along with the binding orientations (SI Table SI1). In all cases the active site is stabilized by an extensive hydrogen bonding network and a hydrophobic pocket created by Val73, Val74, Val116, Phe153, Phe161, Pro162, Phe164, and Ile165. Moreover, significant movement of Phe153/Phe161 and Ile165 is needed to accommodate bulky substituents of HUAs ranging from ethyl to methoxyphenyl groups.

3.1. IFD Results for All HUAs. *N-Hydroxyurea (**1**).* Hydroxyurea, also known as hydroxycarbamide, is used as an antisickling, antineoplastic agent.[50,51] HU has three donors and two acceptors for hydrogen bonding. IFD produced an ensemble of 39 binding orientations for **1**. Two dominant clusters were identified: pose A (15) and pose B (11), while pose AB had only four conformations. Total and decomposed docking scores (Table 1) fell within the known error of GlideXP; therefore, the most favorable pose could not be identified. However, based on populations and a slightly higher docking score for pose AB, it appears less likely compared to pose A and B.

*O-Methyl-N-hydroxyurea (**3**).* This substrate commonly known as 1-methoxyurea contains two donors and two acceptors available for hydrogen bonding. Experimental results indicate that **3** failed to produce NO when interacting with Hb due to the absence of the −NHOH group.[17] IFD produced 83 orientations, but none of the poses can produce C-nitroso formamide due to the lack of −NHOH moiety (Figure 1). The major cluster consisted of 27 docked conformations with the top scoring pose receiving energy stabilization from a unique network of intermolecular hydrogen bonds (SI Figure SI1a) in which the Asn148 $-NH_2$ group interacts with the $-OCH_3$ while the N_ε atom of His75 accepts two hydrogen bonds from H_N and $H_{N'}$. Electrostatic interactions with His75, Asn148, Thr150, and Gln168 also contribute to the stability of **3**.

*N-Methyl-N-hydroxyurea (**4**).* Methyl hydroxyurea has two hydrogen bond donors and two acceptors. **4** produced a nitroxide radical intermediate and had the highest rate constant among the HUAs while interacting with Hb.[17] However, it failed to form NO due to the missing −NHOH group.[18] Similar to **3**, IFD resulted in 80 poses for **4** but did not produce pose A, B, or AB. The major cluster retained 36 docked poses that closely resembled pose A (SI Figure SI1b) but failed to hydrogen bond with the oxoferryl unit. Strong hydrophobic interactions between the $-CH_3$ of **4** and Pro129, Phe153, and Phe154 prevented it from adopting a strict pose A conformation. **4** had a slightly larger LipophilicEvdW contribution than **1** due to the methyl's additional hydrophobic interaction. In this cluster, a slightly modified network of hydrogen bonds existed, in comparison to pose A; here, the interaction of the oxoferryl oxygen with $H_{N'}$ was replaced by $H_{N'}-N_\varepsilon$. **4**'s electrostatic stabilization resulted from interactions with Gln168, Asn148, and His75.

*N′-Phenyl-N-hydroxyurea (**5**).* HUA **5** (1-hydroxy-3-phenylurea) has three hydrogen bond donors and two acceptors. It efficiently released NO upon interacting with hemoglobin and was found to have the second highest rate after **4** in the rate determining step.[17] IFD produced 55 orientations. Clustering showed that pose A and AB were dominant (19 each); whereas, only three poses were assigned to B's cluster. Pose A and AB docked with better GScores compared to pose B. This is primarily due to increased HBond, PhobEnHB, and PhobEn stabilizations in A and AB (Table 1). The PhobEn contribution is attributed to a parallel displaced $\pi-\pi$ stacking interaction between the ligand's phenyl group and the Phe164 side chain, which is absent in pose B. This suggests a possible target for single-point mutation studies; for example, binding kinetics in a F164A mutant should be perturbed significantly if either pose A or AB are preferred. To accommodate this interaction, Ile165

dx.doi.org/10.1021/ci400395c | J. Chem. Inf. Model. 2013, 53, 2951−2961

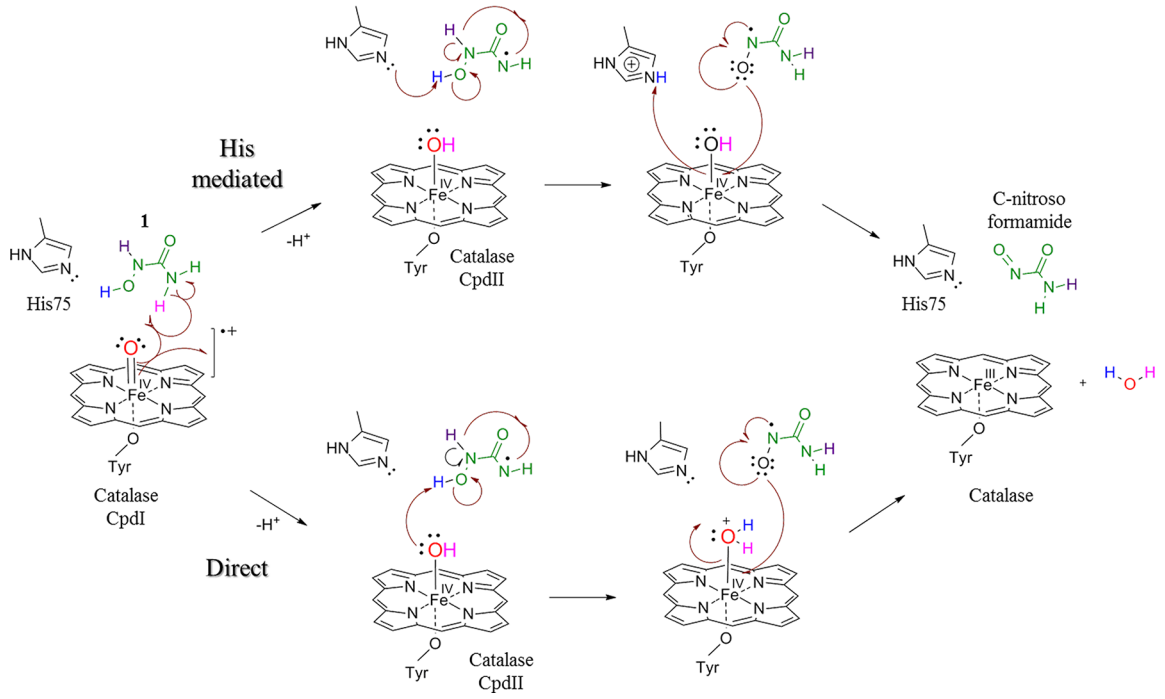

Figure 6. Proposed reaction schemes describing His mediated (top) and direct mechanism (bottom) of actions for HUAs pose A orientations catalyzed by catalase CpdI.

undergoes a torsional rotation confirmed by rmsds of 0.70 and 1.00 Å for pose A and AB, respectively. In general, significant active site rearrangement was needed to bind **5** due to its bulky phenyl substituent. For example, Phe161 moved 2.73, 2.79, and 2.66 Å for pose A, pose B, and pose AB, respectively.

*N′-n-Butyl-N-hydroxyurea (**6**).* This derivative is commonly known as 1-butyl-3-hydroxyurea with three sites for hydrogen bond donation and two acceptors. IFD produced 110 total poses. All three poses for **6** appear to have significant probability; there were 44, 32, and 23 docked poses for A, B, and AB, respectively. Poses A and B have slightly more population and better docking scores than pose AB. This is attributed to a more favorable hydrogen bonding network, which is confirmed by the HBond XP descriptor (Table 1). The RotPenal is similar for all poses (Table 1). This penalty of 1.4 kcal mol^{-1} results from limiting the flexibility of **6**'s *n*-butyl chain in the hydrophobic pocket. This penalty would be larger if not for the flexibility observed in Phe153, Phe161, and Ile165. These significant induced fit effects are illustrated by the rmsd changes respectively for poses A, B, and AB: Phe153 0.05, 2.24, 0.15 Å; Phe161 2.94, 1.37, 2.73 Å; Ile165 0.93, 0.17, 0.60 Å. Phe153/161 rmsd changes are of particular interest as they demonstrate the ability for stabilization of multiple *n*-butyl torsional conformations. Ile165 mirrors this effect.

*N′,N′-Diethyl-N-hydroxyurea (**7**).* This analog is known as 1,1-diethyl 3-hydroxyurea and consists of two donors and two acceptors for hydrogen bonding. **7** was the only HUA that did not produce NO despite having an −NHOH group in Hb.[17] Our previous flexible docking studies, determined that **7**'s inability to form NO was attributed to the absence of the $H_{N'}$ atom.[18] However, this analog may interact with catalase CpdI to produce NO as it contains the essential −NHOH moiety required to form the C-nitroso formamide intermediate. IFD resulted in 22 binding conformations, however, neither pose A nor AB had any representative conformations. Pose B is the preferred binding pose with 16 docked structures. Substrate **7** has a major XP penalty of 2.4 kcal mol^{-1} resulting from the desolvation of the polar NO atom in a hydrophobic protein environment devoid of any hydrogen bonding (Table 1). Similar to IFD results from other bulky HUAs, rmsds (Phe161 2.91 Å; Ile165 0.96 Å) indicated that active site hydrophobic residues must move to accommodate the sizable diethyl substituent.

*N′-4-Methoxy-phenyl-N-hydroxyurea (**8**).* HUA **8** (1-methoxy-3-phenylurea) contains three hydrogen bond donors and three acceptors. Despite this substrate having the potential to release NO while interacting with hemoglobin, experimental studies were not possible due to solubility issues.[17] **8** has the potential to interact with catalase CpdI to produce NO due to the presence of the −NHOH moiety. IFD yielded 60 total poses with 14, 18, and 2 adopting the pose A, B, and AB orientations, respectively. Pose A had better binding affinities largely due to an increased hydrogen bonding contribution (XP Hbond/PhobEnHB) favoring it by −1.9 and −1.4 kcal mol^{-1} in comparison to poses B and AB, respectively (Table 1). This stabilization is attributed to a near perfect hydrogen bonding orientation with Gln168 in contrast to poses B and AB, which are rotated and have a reduced O···H−N angle (vide infra). Again, this suggests a single-point mutation (Q168A) would more significantly perturb the binding kinetics of B/AB compared to A, providing an avenue for experimental validation of our predictions. All poses have a favorable LipophilicEvdW score attributed to hydrophobic interactions between the methoxyphenyl substituent and Val73, Val74, Phe153, Phe161, Phe164, and Ile165. As expected due to the bulky nature of the methoxyphenyl substituent, significant induced fit effects were observed; Phe161 3.2 Å and Ile165 1.2 Å for all poses.

Role of Gln168. Gln168 undergoes an active site rearrangement to provide stabilization via hydrogen bonding for poses A, B, and AB for all HUAs. The Gln168 rearranges to donate a hydrogen bond from its $-NH_2$ side chain to the HUA carbonyl

dx.doi.org/10.1021/ci400395c | J. Chem. Inf. Model. 2013, 53, 2951−2961

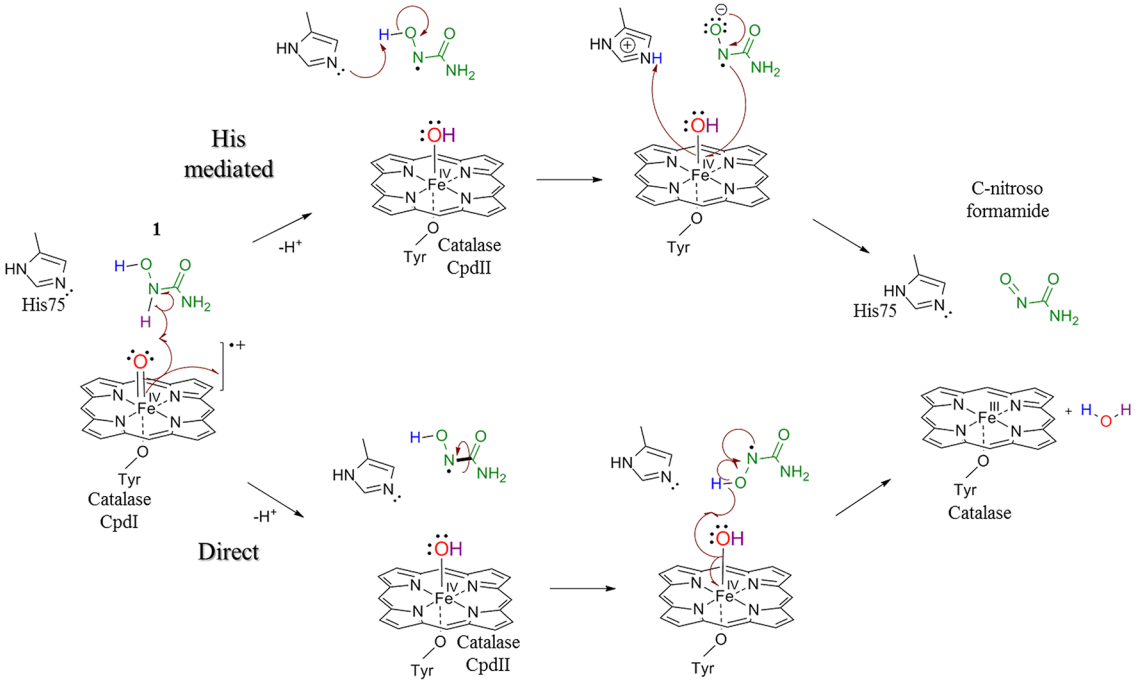

Figure 7. Proposed reaction schemes describing His mediated (top) and direct mechanism (bottom) of actions for HUAs pose B orientations catalyzed by catalase CpdI.

oxygen. This is evident by the average rmsd of 0.67 Å for Gln168 across all poses of all HUAs.

3.2. Proposed Mechanisms of Action. To move beyond binding information, docking and energetic analyses were combined with available structural and experimental data.[13,26,52,53] Careful examination of the pose orientations revealed that His75 could act as both an acid and base catalyst or provide stabilizing hydrogen bonds to the HUA superoxide anion radicals produced during the course of the reaction. On the basis of purely docking studies, a dominant pose cannot be unambiguously assigned; therefore, we propose four possible reaction mechanisms for C-nitroso formamide generation (Figure 3) corresponding to both pose A and B. Although pose AB's initial hydrogen bonding network differs from poses A and B, it was determined that it could not undergo a unique mechanism. Instead, AB would share features of both A and B reactions (vide infra). Analogous to proposed H_2O_2 mechanisms,[26,54] the HU conversion would occur via the reduction of catalase CpdI by either a His mediated or direct mechanism, as the −NHOH moiety of HUA represents an isostere of H_2O_2.

Pose A Mechanisms of Action. The two possible pose A reaction mechanisms are illustrated in Figure 6 (His mediated, top; direct, bottom). In both cases the reaction would most likely be initiated by quenching of the porphyrin cation radical. This would occur by decomposing the double bond of oxoferryl via $H_{N'}$ abstraction; resulting in a radical on N′ and the hydroxy-ferryl unit (CpdII, Figure 6, **2**). This hydrogen abstraction from N′ to the oxoferryl oxygen would be assisted by stabilizing interactions derived from the strong networked intermolecular hydrogen bonds and hydrophobic pocket created by Val74, Val116, Pro129, Phe153, Phe154, Phe161, Phe164, and Ile165. We hypothesize the radical would be localized on the HUA nitrogen rather than oxygen or carbon during this process based on the following evidence. Nitrogen radicals have similar stabilities to oxygen centered radicals due to substituent effects,[55] and they are more stable compared to carbon radicals due to their electron deficient nature.[52] Further, gas phase DFT calculations on **2** by Vrcek et al.[52] showed that N-centered radicals are frequently formed by hydrogen migrations. Calculated Mulliken spin densities showed that an unpaired electron on **2** would likely be located at the O and N_O atoms. It was previously shown using EPR that O-centered radicals (**2**) are the result of **1**'s interaction with human Hb.[17] Nevertheless, these were not observed in **1**'s interaction with catalase, illustrating the feasibility of other radical formations.[13] From previous computational and experimental studies[13,52,55] it is reasonable to expect competition between the H_N and H_O for transfer to the N′ radical. The transfer of the radical (N′ → N_O) is corroborated by the resonance stabilization gained by the N_O radical, due to the lone pair donation from the neighboring oxygen atom. In the subsequent step, the oxygen atom would be deprotonated to generate an oxyanion. This again is supported by Vrcek et al.[52] who showed that **1** behaves as a hydroxamic acid with deprotonation occurring on the O-center to produce an oxyanion. In the His mediated mechanism, it is hypothesized that the His75 N_ε plays a catalytic role to abstract the H_O to produce an oxyanion HUA radical moiety. Further, reduction potential studies indicated that an electron from the oxyanion gets transferred to metal ion oxidants.[52] This observation indicates that the negative charge on the oxygen moiety would dissociate into radicals to quench the N′ radical and transfer the other to Fe^{IV} to form reduced Fe^{III} and C-nitrosoformamide. Finally, the oxygen of the hydroxy-ferryl moiety would deprotonate His75 N_ε proton yielding water. In the case of the direct mechanism (Figure 6), the initial step of the reaction is equivalent to its His mediated counterpart. However, in the second step, HO would be deprotonated by the hydroxy-ferryl group instead of His75 to form an oxonium ion intermediate. Subsequently, the oxyanion charge would be transferred to reduce Fe^{IV} to Fe^{III}, with the oxonium ion leaving the active site as water along with C-nitroso formamide.

dx.doi.org/10.1021/ci400395c | J. Chem. Inf. Model. 2013, 53, 2951−2961

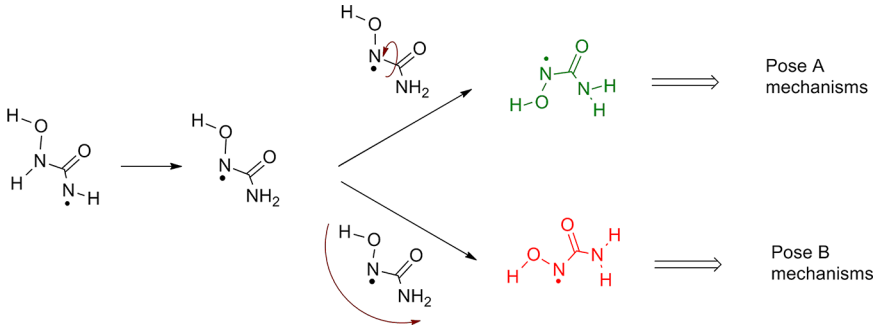

Figure 8. Proposed preorganizational effects and ultimate reaction mechanism for pose AB orientations interacting with catalase CpdI.

Pose B Mechanisms of Action. In the pose B mechanism (Figure 7), all analogs except **3** and **4** retained the same array of intermolecular hydrogen bonds observed in the QM/MM minimized H_2O_2-catalase CpdI complex.[26] This is logical as the −NHOH moiety represents an isostere of H_2O_2. Thus the pose B mechanisms would differ from pose A with respect to hydrogen abstraction and reaction with the oxoferryl moiety. Here, the oxoferryl would abstract the H_N instead of $H_{N'}$ to form CpdI and an N_O centered radical without the intermediacy of the N′ radical rearrangement. The remainder of the His mediated mechanism would mimic therefore that of pose A.

Contrastingly, the pose B direct mechanism would be significantly different. Following the H_N abstraction, the N-centered nitroxide radical would have to reorient itself by rotation around the $C-N_O$ bond to interact with the hydroxyferryl moiety, leading to the reduction of iron, and the formation of C-nitroso formamide. To examine the feasibility of this rearrangement, the torsional potential was calculated ($O-N_O-C-O$) using Q-Chem 4.0[46,47] at the B3LYP/6-31G* level of theory[48,49] with a 75/302 integration grid. The torsion was constrained in 15° increments ranging from −180° to 180°. The torsional profile showed a rotational energy barrier of 6.2 kcal mol^{-1} (SI Figure SI2 and Table SI2) indicating that additional energy would be needed for the pose B direct mechanism. However, this small barrier may be overcome directly or even lowered in the catalytic environment. This reorientation would result in a sequence of N_O radical mediated reactions leading to the formation of C-nitroso formamide and water.

Pose AB Preorganizational Arrangement. As discussed above, pose AB's alternative hydrogen bonding network prevents a feasible mechanism of action without initial rearrangement. This "preorganization" is illustrated in Figure 8. The first step of pose AB's rearrangement is analogous to the first step of the pose A mechanism; the porphyrin cation radical is quenched by decomposing the oxoferryl double bond via $H_{N'}$ abstraction. However, the product differs because the −NHOH hydrogen bonding pattern would still be that of pose AB. Despite the difference in ligand conformation, the radical is likely housed on the N′ for the reasoning discussed in the pose A mechanism. Next, another radical rearrangement would occur that transfers the H_N from N_O to N′.

These preorganizational steps are mandatory for any of the four possible reaction mechanisms to occur starting from pose AB; however, the next step determines whether AB will proceed via the pose A or B mechanistic pathway. To follow the pose A mechanism, the ligand must first undergo a conformational change in which the −NOH radical rotates around the $O-N_O-C-N'$ dihedral (similar to the second step of the pose B direct mechanism). In contrast, if the pose B mechanism is preferred then a rigid body rotation of the ligand must occur where the H_O properly aligns with either the His75 or oxoferryl group (His mediated versus direct mechanism). At this point the preorganization would be complete and C-nitroso formamide could be produced by any of the four mechanisms previously discussed.

Insights into the Role of Catalase CpdI to Decipher the Mechanism of Action of HUAs. IFD resulted in four main reaction mechanisms (Figure 6 and 7) for HUAs. ProBiS,[56−58] a web-based binding site prediction and analysis tool (consisting of 31 198 nonredundant protein structures) was used to compare catalase CpdI to all heme based enzymes. Results showed that the catalase CpdI active site framework is unique. It failed to identify a single heme based protein with similar physiochemical properties; hence, a singular mechanism of action with HUAs is likely.

After examining all HUA docking poses, it was determined that **7** is the only analog that adopts just pose B orientations. This was attributed to the absence of the $H_{N'}$ atom; however, steric clashes between the bulky ethyl groups and active site could also be responsible. To identify the underlying cause, modified analogs of **6** (SI Figure SI3) were generated, in which the $H_{N'}$ was replaced with $-CH_3$ (**6a**) to create a less sterically hindered structure, and $-NH_{N'}$ was replaced with $-CH_2$ (**6b**) to study the importance of the $H_{N'}$ polarity. IFD studies with **6a** and **6b** revealed that pose B is dominant. However, unlike **7** "pose A-like" conformations (SI Figure SI4) were observed for both **6a** and **6b** with only **6b** adopting a "pose AB-like" orientation. This suggests that **7**'s inability to adopt pose A- and AB-like conformations is as much due to steric hindrance as it is to the absence of $H_{N'}$. Thus, CpdI should be able to react with **6a**, **6b**, and **7** to produce NO as they all contain the necessary −NHOH moiety. These conclusions are supported by previous spectroscopic studies that showed hydroxylamine (NH_2OH) produces HNO upon reaction with catalase CpdI (SI Figure SI5).[53] This suggests that substrates containing just −NHOH are sufficient to produce NO due to the isosteric relationship with H_2O_2. Moreover, hydroxylamine was shown to have a similar reaction profile to **1**, as confirmed by EPR spectra.[53] To examine this in atomistic detail, we docked (with IFD) hydroxylamine; as expected, this resulted only in the pose B orientation.

In general, small molecules with an −NHOH group should produce HNO even if no $H_{N'}$ or amide functional group exists. It is unclear which pose would be preferred in the binding and reaction, but likely this is tunable as a function of substituent. On the basis of homology to the native substrate, it is

reasonable to expect pose B conformations to be favored over pose A or AB. Further, due to the small rotational barrier implicit to the pose B direct mechanism, it is likely that His75 would play an active catalytic role. Experimental and QM/MM studies will be needed to elucidate the correct mechanism; the later are currently underway.

4. CONCLUSIONS

The pharmacological efficacy of HU therapy results from NO production, ultimately leading to elevation of fetal Hb levels, vasodilation, and prevention of sickle cell adhesion to endothelium cells. Previous work in our lab has focused on correlating experimental SAR studies of the hemoglobin catalyzed production of NO to structural and mechanistic information.[18] This was the first step in our long-term goal of elucidating the binding and mechanistic detail of enzymes primarily responsible for in vivo conversion of HU → NO. Catalase CpdI is such an enzyme, known to produce NO upon interacting with HU and lacking characterization of its binding and reaction mechanism.

Presently, we examined nine HU analogs (HUAs), including modified analogs complexed with catalase CpdI using induced fit docking (IFD) coupled with scoring function decomposition. Our work revealed an important network of intermolecular hydrogen bonds created by distal residues His75, Asn148, Gln168, and oxoferryl-heme to HUAs. Also, strong hydrophobic interactions exist between substrates and active site residues Val73, Val74, Val116, Phe153, Phe161, Pro162, Phe164, and Ile165. Further, Phe153/Phe161 undergoes significant induced fit effects to accommodate aromatic substrates like **5** and **8**. We proposed reaction mechanisms using information obtained from predicted binding modes coupled with available biochemical data.

Bioinformatics results obtained via binding site analysis (i.e ProBiS) indicated that catalase CpdI could have a unique mechanism of action compared to nearly all heme based enzymes. Moreover, the similarities in structural, physiochemical, and biological action between hydroxyurea, hydroxylamine, and hydrogen peroxide confirm the likelihood of the pose B reaction pathways. Further, the pose B His mediated pathway seems to have slightly higher probability of occurrence due to the small rotational energy barrier needed in the direct mechanism. Further analysis of **6a**, **6b**, **7**, and hydroxylamine suggested that a −NHOH moiety, an isostere to H_2O_2, is all that is necessary to produce NO. Structural and mechanistic details of HUAs and catalase CpdI should serve as a model for continued mechanistic studies and ideally structure based drug design. Specifically, targeting new scaffolds with −NHOH as the base pharmacophore could be an excellent plan of action moving forward in the development of a new sickle cell disease treatment.

■ ASSOCIATED CONTENT

Supporting Information

Binding orientations of **3** and **4**, full plot of **1**'s torsional potential (and data), Chemdraw figures of **6a** and **6b**, possible binding orientations of **6b**, reaction schematic of hydroxylamine with catalase, and summary of IFD refinement binding orientations. This material is available free of charge via the Internet at http://pubs.acs.org.

■ AUTHOR INFORMATION

Corresponding Author

*E-mail: hlw@usf.edu.

Notes

The authors declare no competing financial interest.

■ ACKNOWLEDGMENTS

The authors would like to thank Professors Wayne Guida, Randy Larsen, and Peter Zhang for their helpful discussions. H.L.W.3 would like to acknowledge the NIH (1K22HL088341-01A1) and the University of South Florida (start-up) for funding. Further, computational resources provided by USF Research Computing (under NSF grant no. CHE-0722887) and XSEDE (grant no. MCB120133) are also greatly appreciated.

■ REFERENCES

(1) Frenette, P. S.; Atweh, G. F. Sickle cell disease: old discoveries, new concepts, and future promise. *J. Clin. Invest.* **2007**, *117*, 850−858.
(2) Chiang, E. Y.; Frenette, P. S. Sickle cell vaso-occlusion. *Hematol. Oncol. Clin. North. Am.* **2005**, *19*, 771−784.
(3) Colombatti, R.; Maschietto, N.; Varotto, E.; Grison, A.; Grazzina, N.; Meneghello, L.; Teso, S.; Carli, M.; Milanesi, O.; Sainati, L. Pulmonary hypertension in sickle cell disease children under 10 years of age. *Br. J. Hamaetol.* **2010**, *150*, 601−609.
(4) Stuart, M. J.; Setty, B. N. Y. Sickle cell acute chest syndrome: pathogenesis and rationale for treatment. *Blood* **1999**, *94*, 1555−1560.
(5) Lanzkron, S.; Haywood, C. J.; Hassell, K. L.; Rand, C. Provider barriers to hydroxyurea use in adults with sickle cell disease: a survey of the sickle cell disease adult provider network. *J. Natl. Med. Assoc.* **2008**, *100*, 968−973.
(6) Strouse, J. J.; Lanzkron, S.; Beach, M. C.; Haywood, C.; Park, H.; Witkop, C.; Wilson, R. F.; Bass, E. B.; Segal, J. B. Hydroxyurea for sickle cell disease: a systematic review for efficacy and toxicity in children. *Pediatrics* **2008**, *122*, 1332−1342.
(7) Steinberg, M. H.; Lu, Z. H.; Barton, F. B.; Terrin, M. L.; Charache, S.; Dover, G. J. Fetal hemoglobin in sickle cell anemia: determinants of response to hydroxyurea. multicenter study of hydroxyurea. *Blood* **1997**, *89*, 1078−1088.
(8) Steinberg, M. H.; Barton, F.; Castro, O.; Pegelow, C. H.; Ballas, S. K.; Kutlar, A.; Orringer, E.; Bellevue, R.; Olivieri, N.; Eckman, J.; Varma, M.; Ramirez, G.; Adler, B.; Smith, W.; Carlos, T.; Ataga, K.; DeCastro, L.; Bigelow, C.; Saunthararajah, Y.; Telfer, M.; Vichinsky, E.; Claster, S.; Shurin, S.; Bridges, K.; Waclawiw, M.; Bonds, D.; Terrin, M. Effect of hydroxyurea on mortality and morbidity in adult sickle cell anemia: risks and benefits up to 9 years of treatment. *JAMA: J. Am. Med. Assoc.* **2003**, *289*, 1645−1651.
(9) Ikuta, T.; Ausenda, S.; Cappellini, M. D. Mechanism for fetal globin gene expression: role of the soluble guanylate cyclase-cgmp-dependent protein kinase pathway. *Proc. Natl. Acad. Sci. U.S.A.* **2001**, *983*, 1847−1852.
(10) Cokic, V. P.; Smith, R. D.; Beleslin-Cokic, B. B.; Njoroge, J. M.; Miller, J. L.; Gladwin, M. T.; Schechter, A. N. Hydroxyurea induces fetal hemoglobin by the nitric oxide-dependent activation of soluble guanylyl cyclase. *J. Clin. Invest.* **2003**, *111*, 231−239.
(11) Silva, D. G. H.; Belini, E. J.; Torres, L. d. S.; Ricci, O. J.; Lobo, C. d. C.; Bonini-Domingos, C. R.; Alves de Almeida, E. Relationship between oxidative stress, glutathione s-transferase polymorphisms and hydroxyurea treatment in sickle cell anemia. *Blood Cells. Mol. Dis.* **2011**, *47*, 23−28.
(12) King, S. B. Mechanisms and novel directions in the biological applications of nitric oxide donors. *Free Radic. Biol. Med.* **2004**, *37*, 735−736.
(13) Huang, J.; Kim-Shapiro, D. B.; King, S. B. Catalase-mediated nitric oxide formation from hydroxyurea. *J. Med. Chem.* **2004**, *47*, 3495−3501.

(14) Huang, J.; Sommers, E. M.; Kim-Shapiro, D. B.; King, S. B. Horseradish peroxidase catalyzed nitric oxide formation from hydroxyurea. *J. Am. Chem. Soc.* **2002**, *124*, 3473−3480.
(15) Juul, T.; Malolepszy, A.; Dybkaer, K.; Kidmose, R.; Rasmussen, J. T.; Andersen, G. R.; Johnsen, H. E.; Jorgensen, J.-E.; Andersen, S. U. The in vivo toxicity of hydroxyurea depends on its direct target catalase. *J. Biol. Chem.* **2010**, *285*, 21411−21415.
(16) Rupon, J. W.; Domingo, S. R.; Smith, S. V.; Gummadi, B. K.; Shields, H.; Ballas, S. K.; King, S. B.; Kim-Shapiro, D. B. The reactions of myoglobin, normal adult hemoglobin, sickle cell hemoglobin and hemin with hydroxyurea. *Biophys. Chem.* **2000**, *84*, 1−11.
(17) Huang, J.; Zou, Z.; Kim-Shapiro, D. B.; Ballas, S. K.; King, S. B. Hydroxyurea analogues as kinetic and mechanistic probes of the nitric oxide producing reactions of hydroxyurea and oxyhemoglobin. *J. Med. Chem.* **2003**, *46*, 3748−3753.
(18) Vankayala, S. L.; Hargis, J. C.; Woodcock, H. L. Unlocking the binding and reaction mechanism of hydroxyurea substrates as biological nitric oxide donors. *J. Chem. Inf. Model.* **2012**, *52*, 1288−1297.
(19) Goyal, M. M.; Basak, A. Human catalase: looking for complete identity. *Protein Cell.* **2010**, *1*, 888−897.
(20) Fernandez-Lafuente, R. Stabilization of multimeric enzymes: Strategies to prevent subunit dissociation. *Enzyme Microb. Technol.* **2009**, *45*, 405−418.
(21) Wood, K. C.; Granger, D. N. Sickle cell disease: role of reactive oxygen and nitrogen metabolites. *Clin. Exp. Pharmacol. Physiol.* **2007**, *34*, 926−932.
(22) Rovira, C.; Alfonso-Prieto, M.; Biarnes, X.; Carpena, X.; Fita, I.; Loewen, P. C. A first principles study of the binding of formic acid in catalase complementing high resolution x-ray structures. *Chem. Phys.* **2006**, *323*, 129−137.
(23) Fita, I.; Rossmann, M. G. The active center of catalase. *J. Mol. Biol.* **1985**, *185*, 21−37.
(24) Kato, S.; Ueno, T.; Fukuzumi, S.; Watanabe, Y. Catalase reaction by myoglobin mutants and native catalase: Mechanistic investigation by kinetic isotope effect. *J. Biol. Chem.* **2004**, *279*, 52376−52381.
(25) Putnam, C. D.; Arvai, A. S.; Bourne, Y.; Tainer, J. A. Active and inhibited human catalase structures: Ligand and nadph binding and catalytic mechanism. *J. Mol. Biol.* **2000**, *296*, 295−309.
(26) Alfonso-Prieto, M.; Biarnes, X.; Vidossich, P.; Rovira, C. The molecular mechanism of the catalase reaction. *J. Am. Chem. Soc.* **2009**, *131*, 11751−11761.
(27) Banks, J. L.; Beard, H. S.; Cao, Y.; Cho, A. E.; Damm, W.; Farid, R.; Felts, A. K.; Halgren, T. A.; Mainz, D. T.; Maple, J. R.; Murphy, R.; Philipp, D. M.; Repasky, M. P.; Zhang, L. Y.; Berne, B. J.; Friesner, R. A.; Gallicchio, E.; Levy, R. M. Integrated modeling program, applied chemical theory (impact). *J. Comput. Chem.* **2005**, *26*, 1752−1780.
(28) *Ligprep*, version 2.3; Schrodinger, LLC.: New York, 2009.
(29) Sherman, W.; Day, T.; Jacobson, M. P.; Friesner, R. A.; Farid, R. Novel procedure for modeling ligand/receptor induced fit effects. *J. Med. Chem.* **2006**, *49*, 534−553.
(30) Sherman, W.; Beard, H. S.; Farid, R. Use of an induced fit receptor structure in virtual screening. *Chem. Biol. Drug Des.* **2006**, *67*, 83−84.
(31) Friesner, R. A.; Murphy, R. B.; Repasky, M. P.; Frye, L. L.; Greenwood, J. R.; Halgren, T. A.; Sanschagrin, P. C.; Mainz, D. T. Extra precision glide: Docking and scoring incorporating a model of hydrophobic enclosure for protein-ligand complexes. *J. Med. Chem.* **2006**, *49*, 6177−6196.
(32) Jacobson, M. P.; Pincus, D. L.; Rapp, C. S.; Day, T. J. F.; Honig, B.; Shaw, D. E.; Friesner, R. A. A hierarchical approach to all-atom protein loop prediction. *Proteins: Struct., Funct., Bioinf.* **2004**, *55*, 351−367.
(33) Coutsias, E. A.; Seok, C.; Jacobson, M. P.; Dill, K. A. A kinematic view of loop closure. *J. Comput. Chem.* **2004**, *25*, 510−528.
(34) McRobb, F. M.; Capuano, B.; Crosby, I. T.; Chalmers, D. K.; Yuriev, E. Homology modeling and docking evaluation of aminergic g protein-coupled receptors. *J. Chem. Inf. Model.* **2010**, *50*, 626−637.
(35) Babaoglu, K.; Shoichet, B. K. Deconstructing fragment-based inhibitor discovery. *Nat. Chem. Biol.* **2006**, *2*, 720−723.
(36) Gadakar, P. K.; Phukan, S.; Dattatreya, P.; Balaji, V. N. Pose prediction accuracy in docking studies and enrichment of actives in the active site of gsk-3. *J. Chem. Inf. Model.* **2007**, *47*, 1446−1459.
(37) Felts, A. K.; LaBarge, K.; Bauman, J. D.; Patel, D. V.; Himmel, D. M.; Arnold, E.; Parniak, M. A.; Levy, R. M. Identification of alternative binding sites for inhibitors of hiv-1 ribonuclease h through comparative analysis of virtual enrichment studies. *J. Chem. Inf. Model.* **2011**, *51*, 1986−1998.
(38) Friesner, R. A.; Banks, J. L.; Murphy, R. B.; Halgren, T. A.; Klicic, J. J.; Mainz, D. T.; Repasky, M. P.; Knoll, E. H.; Shelley, M.; Perry, J. K.; Shaw, D. E.; Francis, P.; Shenkin, P. S. Glide: A new approach for rapid, accurate docking and scoring. 1. method and assessment of docking accuracy. *J. Med. Chem.* **2004**, *47*, 1739−1749.
(39) Jacobson, M. P.; Friesner, R. A.; Xiang, Z.; Honig, B. On the role of the crystal environment in determining protein side-chain conformations. *J. Mol. Biol.* **2002**, *320*, 597−608.
(40) Jacobson, M. P.; Kaminski, G. A.; Friesner, R. A.; Rapp, C. S. Force field validation using protein side chain prediction. *J. Phys. Chem. B* **2002**, *106*, 11673−11680.
(41) Xiang, Z.; Honig, B. Extending the accuracy limits of prediction for side-chain conformations. *J. Mol. Biol.* **2001**, *311*, 421−430.
(42) Eldridge, M. D.; Murray, C. W.; Auton, T. R.; Paolini, G. V.; Mee, R. P. Empirical scoring functions: I. the development of a fast empirical scoring function to estimate the binding affinity of ligands in receptor complexes. *J. Comput.-Aided Mater. Des.* **1997**, *11*, 425−445.
(43) Miller, B. T.; Singh, R. P.; Klauda, J. B.; Hodoscek, M.; Brooks, B. R.; Woodcock, H.; Lee, I. Charmming: A new, flexible web portal for charmm. *J. Chem. Inf. Model.* **2008**, *48*, 1920−1929.
(44) Brooks, B. R.; Brooks, I. C. L.; Mackerell, J. A. D.; Nilsson, L.; Petrella, R. J.; Roux, B.; Won, Y.; Archontis, G.; Bartels, C.; Boresch, S.; Caflisch, A.; Caves, L.; Cui, Q.; Dinner, A. R.; Feig, M.; Fischer, S.; Gao, J.; Hodoscek, M.; Im, W.; Kuczera, K.; Lazaridis, T.; Ma, J.; Ovchinnikov, V.; Paci, E.; Pastor, R. W.; Post, C. B.; Pu, J. Z.; Schaefer, M.; Tidor, B.; Venable, R. M.; Woodcock, H. L.; Wu, X.; Yang, W.; York, D. M.; Karplus, M. Charmm: The biomolecular simulation program. *J. Comput. Chem.* **2009**, *30*, 1545−1614.
(45) Brooks, B. R.; Bruccoleri, R. E.; Olafson, B. D.; States, D. J.; Swaminathan, S.; Karplus, M. Charmm: a program for macromolecular energy, minimization, and dynamics calculations. *J. Comput. Chem.* **1983**, *4*, 187−217.
(46) Kong, J.; White, C. A.; Krylov, A. I.; Sherrill, D.; Adamson, R. D.; Furlani, T. R.; Lee, M. S.; Lee, A. M.; Gwaltney, S. R.; Adams, T. R.; Ochsenfeld, C.; Gilbert, A. T. B.; Kedziora, G. S.; Rassolov, V. A.; Maurice, D. R.; Nair, N.; Shao, Y.; Besley, N. A.; Maslen, P. E.; Dombroski, J. P.; Daschel, H.; Zhang, W.; Korambath, P. P.; Baker, J.; Byrd, E. F. C.; Van Voorhis, T.; Oumi, M.; Hirata, S.; Hsu, C.-P.; Ishikawa, N.; Florian, J.; Warshel, A.; Johnson, B. G.; Gill, P. M. W.; Head-Gordon, M.; Pople, J. A. Q-chem 2.0: a high-performance ab initio electronic structure program package. *J. Comput. Chem.* **2000**, *21*, 1532−1548.
(47) Woodcock, H.; Lee, I.; Hodoscek, M.; Gilbert, A. T. B.; Gill, P. M. W.; Schaefer, H. F. I.; Brooks, B. R. Interfacing q-chem and charmm to perform qm/mm reaction path calculations. *J. Comput. Chem.* **2007**, *28*, 1485−1502.
(48) Becke, A. D. A new mixing of hartree-fock and local-density-functional theories. *J. Chem. Phys.* **1993**, *98*, 1372−1377.
(49) Lee, C.; Yang, W.; Parr, R. G. Development of the colle-salvetti correlation-energy formula into a functional of the electron density. *Phys. Rev. B* **1988**, *37*, 785−9.
(50) McGann, P. T.; Ware, R. E. Hydroxyurea for sickle cell anemia: what have learned and what questions still remain? *Curr. Opin. Hematol.* **2011**, *18*, 158−165.
(51) Karimi, M.; Zekavat, O. R.; Sharifzadeh, S.; Mosavizadeh, K. Clinical response of patients with sickle cell anemia to cromolyn sodium nasal spray. *Am. J. Hematol.* **2006**, *81*, 809−816.

(52) Vrcek, I. V.; Sakic, D.; Vrcek, V.; Zipse, H.; Birus, M. Computational study of radicals derived from hydroxyurea and its methylated analogues. *Org. Biomol. Chem.* **2012**, *10*, 1196−1206.
(53) Donzelli, S.; Espey, M. G.; Flores-Santana, W.; Switzer, C. H.; Yeh, G. C.; Huang, J.; Stuehr, D. J.; King, S. B.; Miranda, K. M.; Wink, D. A. Generation of nitroxyl by heme protein-mediated peroxidation of hydroxylamine but not n-hydroxy-l-arginine. *Free Radic. Biol. Med.* **2008**, *45*, 578−584.
(54) Alfonso-Prieto, M.; Vidossich, P.; Rovira, C. The reaction mechanisms of heme catalases: An atomistic view by ab initio molecular dynamics. *Arch. Biochem. Biophys.* **2012**, *525*, 121−130.
(55) Zipse, H. Radical stability - a theoretical perspective. *Top. Curr. Chem.* **2006**, *263*, 163−189.
(56) Konc, J.; Cesnik, T.; Konc, J. T.; Penca, M.; Janezic, D. Probis-database: Precalculated binding site similarities and local pairwise alignments of pdb structures. *J. Chem. Inf. Model.* **2012**, *52*, 604−612.
(57) Konc, J.; Janezic, D. Probis: a web server for detection of structurally similar protein binding sites. *Nucleic Acids Res.* **2010**, *38*, W436−W440.
(58) Konc, J.; Janezic, D. Probis algorithm for detection of structurally similar protein binding sites by local structural alignment. *Bioinformatics* **2010**, *26*, 1160−1168.